SECTION COPY

UNCLASSIFIED

Copy 480



NASA TM X-157

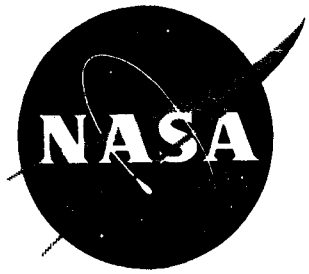


GROUP 1
Excluded from automatic
downgrading and declassification

# TECHNICAL MEMORANDUM X-157

## MEASUREMENTS OF TRANSONIC FLUTTER DERIVATIVES FOR A MIDSPAN CONTROL SURFACE ON A MODIFIED DELTA WING

By John A. Wyss, Robert M. Sorenson, and
Bruno J. Gambucci

Ames Research Center
Moffett Field, Calif.

CLASSIFICATION CHANGED TO UNCLASSIFIED
BY AUTHORITY OF NASA CLASSIFICATION CHANGE
NOTICES, CHANGE NO. 209-25. EFF. 10/19/70
JR

CLASSIFIED DOCUMENT - TITLE UNCLASSIFIED

This material contains information affecting the national defense of the United States within the meaning of the espionage laws, Title 18, U.S.C., Secs. 793 and 794, the transmission or revelation of which in any manner to an unauthorized person is prohibited by law.

NATIONAL AERONAUTICS AND SPACE ADMINISTRATION

WASHINGTON January 1960

UNCLASSIFIED

16999

UNCLASSIFIED

1L

NATIONAL AERONAUTICS AND SPACE ADMINISTRATION

TECHNICAL MEMORANDUM X-157

# MEASUREMENTS OF TRANSONIC FLUTTER DERIVATIVES FOR A MIDSPAN CONTROL SURFACE ON A MODIFIED DELTA WING*

By John A. Wyss, Robert M. Sorenson, and
Bruno J. Gambucci

A-200

## SUMMARY

Transonic flutter derivatives were determined for representative sections of a midspan control surface mounted on a modified delta wing with hinge line perpendicular to the wind stream. The control was also tested with triangular-shaped wedges, superposed along the control surface.

The plain control surface encountered unstable aerodynamic damping moments at about 0.91 Mach number after the shock position moved back onto the control surface. Effects of frequency were secondary. The addition of wedges delayed instability to a higher Mach number, but did not eliminate an abrupt loss in damping. Results for the modified delta wing were quite similar to those for a straight wing on which the same control surface had been previously tested.

## INTRODUCTION

Transonic control-surface flutter derivatives for a variety of control-surface configurations on a 6-percent-thick straight wing of aspect ratio 3 were presented in reference 1. The mechanism for flutter for a plain control appeared to be associated with the presence of shock waves on the control surface, and in particular, although possibly coincidental, unstable damping derivatives were encountered when the shock wave crossed the hinge line as Mach number approached unity. This result was in essential agreement to that found in references 2 and 3. However, these results may not necessarily preclude the possibility that this type of flutter can occur without the presence of shock waves.

*Title, Unclassified

UNCLASSIFIED

A
.2
0
0

In order to determine whether large changes in wing geometry would appreciably alter the flutter characteristics of the control surface, the 6-percent-thick straight-wing portion of the model of reference 1 was replaced with a modified delta plan form having a wing thickness-chord ratio of 0.017 at the root. Previous investigations of oscillatory flap hinge moments on delta wings are described in references 4, 5, and 6. Since wedges superposed on the control surface of the straight wing had delayed instability to a higher Mach number, several wedge configurations were also investigated on the delta wing. All control-surface flutter derivatives were obtained at an amplitude of $\pm 1.08^{\circ}$, so that comparisons could be made at an identical amplitude of oscillation. Angle of attack and mean angle of flap deflection were limited to $0^{\circ}$.

## SYMBOLS

$b$ local wing semichord, ft

$c_b$ balance chord (distance from hinge line to leading edge of control), ft

$c_f$ control chord (distance from hinge line to trailing edge), ft

$c_h$ control hinge-moment coefficient, $\frac{HM}{(1/2)\rho V^2 c_t^2}$

$c_{h_\delta}$ $\frac{\partial c_h}{\partial \delta}$, per radian

$c_{h_{\dot{\delta}}}$ aerodynamic damping-moment coefficient, $\frac{\partial c_h}{\partial(\dot{\delta} b/V)}$

$c_t$ total control chord, $c_b + c_f$, ft

$f$ frequency, cps

HM hinge moment per unit span, ft-lb/ft

$k$ reduced frequency, $\frac{\omega b}{V}$, with $b$ taken at 3/8 semispan

$M$ Mach number, $\frac{V}{\text{speed of sound}}$

$V$ velocity of air stream, ft/sec

$\delta$ control-surface deflection angle, radians except where noted

$\dot{\delta}$ control-surface angular velocity, $\frac{d\delta}{dt}$, radians/sec

$\theta$ phase angle of resultant aerodynamic moment with respect to control displacement, deg

$\rho$ density of air stream, slugs/cu ft

$\omega$ angular frequency, $2\pi f$, radians/sec

## APPARATUS

The experimental methods and techniques were similar to those used in reference 1. Since detailed descriptions of the tunnel, control-surface drive system, and instrumentation are presented therein, only the more salient features will be described.

### Tunnel, Model, and Control Surfaces

The present investigation was conducted in the Ames 14-foot transonic wind tunnel. A sectional sketch of the tunnel is shown in figure 1. Figure 2 shows the model mounted in the test section. The model passed through a wood filler block in the floor and was bolted to the floor understructure. Vortex generators installed at the upstream end of the test section were found to minimize boundary-layer thickness at the model without introducing fluctuations in the free stream. A small leading-edge fence was mounted near the root of the model to prevent low-energy air from bleeding up the leading edge.

Model dimensions are shown in figure 3. The modified delta wing had a uniform thickness section with beveled leading and trailing edges. The wing thickness-chord ratio was 0.017 at the root, and 0.025 at midspan. This ratio is not constant because of the use of the instrumented control surface used in reference 1 which determined wing thickness taper.

In order to provide additional stiffness and damping, a 5/32-inch aircraft cable was passed through a plastic block near the wing tip, sweptback about $20^{\circ}$, and attached to a cantilever spring system outside of the wind tunnel. The cable enabled the control surface to be safely oscillated up to 30 cps with negligible coupling between the control surface and wing.

A detailed view of the control surface with superposed triangular wedges or tetrahedra is shown in figure 4. The nose portion of the basic control surface was derived from an NACA 2-006 profile. A blunt trailing edge of 0.2-inch thickness was used to facilitate pressure-cell installation at the trailing edge. Chordwise rows of pressure cells and pressure

orifices were installed at 3/8 and 5/8 of the wing semispan. The control-surface hinge line was perpendicular to the free-stream direction and was located to provide a 0.40 balance chord to flap chord ratio, based on mean aerodynamic chord of the flap.

The wedges shown in figure 4 have an included angle between adjacent wedges of about 30°, and extend from the point of maximum thickness to the trailing edge. The ramp angle relative to the wind stream was 3.6°. Wedges with 0° ramp angle (trailing-edge thickness equal to flap maximum thickness) were also investigated. Wedges with an included angle of 15° between adjacent wedges having ramp angles of 0° or 7.2° were also investigated.

## Control-Surface Drive System

A schematic drawing of the mechanical details of the drive system is illustrated in figure 5. A closed-loop servo system controlled the mean angle of deflection, amplitude, and frequency of the control surface. The control-surface motion was measured with a slide-wire position transducer which was attached to the sector arm shown in figure 5. All data have been referenced to this positioner, since tests indicated that negligible errors in phase angle were introduced by the torsional deflection of the control surface and torque shaft.

## Instrumentation

The electrical responses from nine pairs of cells were summed electronically to provide a signal proportional to the flap dynamic hinge moment. This signal and the position transducer signal were simultaneously recorded on magnetic tape and used as inputs to the NASA Ames flutter analyzer. Meter readings of the following quantities were obtained: root mean square amplitude of control-surface motion, rms amplitude of the oscillatory hinge moment, and the phase angle between the fundamental components of the two inputs at the frequency at which the control surface was oscillated. A meter reading proportional to the aerodynamic damping component was also obtained. With Mach number and wing angle of attack constant, data were taken for time intervals of about 30 seconds at each frequency. Due to the unsteadiness of meter readings at Mach numbers near that at which the damping component changed sign, time-average readings were recorded for 30-second time intervals. In view of this unsteadiness, the over-all accuracy is estimated to be on the order of 5 percent for magnitude, and ±3° in phase angle. It should be kept in mind that the data are statistical in nature in that the time-average readings are for not less than 300 cycles.

Since the data were obtained for two control-surface stations, it should be noted that the derivatives are sectional, rather than total control-surface hinge-moment derivatives. As also noted in reference 1, spanwise effects were negligible, so that the results are presumed to be representative for the entire control surface, even though end effects are neglected. However, such a two-dimensional treatment of the data for the wedge configurations is open to question because of the obvious three-dimensional type of disturbances that would be generated by the wedges. Detailed results for the wedge configurations are therefore omitted.

### Shadowgraphs

A mercury vapor lamp powered by 1200 volts d.c. was used as a point light source. The lamp was mounted directly in line with the flap leading edge at a sufficient height so that a ray of light traveled along the trailing edge. The light source was above the tunnel ceiling and the presence of shock waves was indicated by shadows on the tunnel floor. A motion-picture camera, operated at 300 frames per second, was mounted adjacent to the light source to record shock-wave motion and position.

## SCOPE OF TESTS

Control-surface flutter derivatives for representative sections were obtained for the various configurations for a wing angle of attack of $0^\circ$ and for a mean angle of control-surface deflection of $0^\circ$ for Mach numbers from 0.6 to 1.13. Reynolds numbers based on wing mean aerodynamic chord varied from 25.2 to 33.2 million. The control surface was oscillated at an amplitude of $\pm 1.08^\circ$ at frequencies from 10 to 30 cps.

## RESULTS AND DISCUSSION

The measured flutter derivatives for the plain control surface are presented in table I. Tabulated values have been cross-plotted to obtain derivatives at constant reduced frequency and are presented as a function of Mach number in figure 6. Results of an analysis of the high-speed motion-picture shadowgraphs to determine shock-wave location as a function of Mach number for the plain control surface are presented in figure 7. The present results for the plain control surface are compared with those for a straight wing in figure 8.

[redacted]

## Plain Control Surface

It is apparent from figure 6 that the general trends for the parameters shown for each reduced frequency are quite similar. The abrupt loss in damping resulting in unstable aerodynamic damping coefficients near 0.91 Mach number (fig. 6(b)) appears to be a typical characteristic for each reduced frequency. This result is in general agreement with a previous wind-tunnel investigation of a cropped delta wing reported in reference 4, and with a free-flight investigation reported in reference 5. In the former (ref. 4) an abrupt loss in damping occurred at a Mach number of about 0.98 with a reduced frequency, k, of 0.13, while in the latter (ref. 5) the sudden loss in damping occurred near 0.93 Mach number for a reduced frequency, k, of 0.17.

Previous analysis of shadowgraph data for a straight wing (ref. 1) had indicated that the Mach number for instability coincided with the Mach number at which the compression shock wave crossed the hinge line of the control surface. Analysis of the data for the delta wing, presented in figure 7, leads to the same conclusion. It may be noted that shock-wave travel reduces during flap oscillation as Mach number approaches 1.

The simplicity of the shock-wave pattern during flap oscillation, consisting of an expansion wave near the flap leading edge, and a normal shock oscillating on the flap surface, might suggest the use of shock-wave position as a criterion for the onset of instability for a plain control surface. However, it should be pointed out that for an angle of attack, the shock pattern can be quite different, so that the results in figure 7 are typical only for an angle of attack of $0^\circ$. Nevertheless, the results in figure 7 appear to indicate that the flutter mechanism, as for the straight wing, is associated with shock-wave position and motion. As previously noted, these results may not necessarily preclude the possibility that single-degree-of-freedom flutter might occur without the presence of shock waves.

## Wedges

The addition of wedges with $0^\circ$ ramp angle had little effect whether the included angle between wedges was $30^\circ$ or $15^\circ$. Increasing the ramp angle (for either wedge angle) delayed instability to about 0.97 Mach number but did not eliminate an abrupt loss in damping similar to that shown in figure 6(b). The slight increase from 0.92 to 0.97 in the Mach number for instability would be at the expense of a large drag increase (see ref. 7).

[redacted]

## Plan Form

Results for the plain control surface on two different plan forms are illustrated in figure 8. It is perhaps of interest to note that the advantages one might expect from such a highly swept plan form as the modified delta wing were not realized in that instability occurred at a lower, rather than a higher, Mach number. It was found in reference 8, that flutter could be delayed on a thick cambered straight wing by successively increasing the sweep angle and the sweep angle of the hinge line by rotating the wing tip downstream. Formation of shock waves at maximum thickness on a line well ahead of the hinge line, along with a reduction in the velocity normal to the hinge line due to sweep effects, could have the effect of delaying the rearward travel of the shock wave to a higher Mach number and, hence, increase the flutter speed. In contrast, when one considers boundary-layer growth on the thin delta wing of the present investigation, the effective line of maximum thickness with flap deflected could be expected to be at the flap leading edge which, in the present instance, is normal to the free stream. The shock wave would then contact the flap at a lower Mach number. It thus appears that the expected advantages of sweep, at least for the control-surface flutter case, are not necessarily present on a thin delta wing with hinge line normal to free-stream velocity. These considerations do not seem unreasonable in that instability of the control surface on the delta wing having an NACA 65A006 profile in reference 5 occurred at a slightly higher Mach number of about 0.93, while for the delta wing in reference 4, which had maximum thickness far forward with a highly swept line of maximum thickness, the control surface did not encounter instability until a Mach number of about 1.02 was reached. Nevertheless, it appears that a large reduction in wing thickness, and a drastic change in plan form from that of the straight wing did not appreciably alter the measured derivatives or have a large effect on the basic mechanism for control-surface flutter at transonic speeds.

## CONCLUSIONS

The results of the experimental investigation of the dynamic hinge-moment characteristics for representative sections of a midspan control surface with an unswept hinge line on a modified delta wing can be summarized as follows:

1. For the range of frequencies under investigation, the effects of reduced frequency were secondary in nature for the delta plan form.

2. The use of a thin delta plan form with uniform thickness section does not appreciably alter the basic problem of single-degree-of-freedom control-surface flutter at transonic speeds.

3. By the addition of triangular-shaped wedges to the control surface, instability could be delayed to a higher subsonic Mach number. However, a characteristic sudden loss in damping could not be eliminated.

Ames Research Center
National Aeronautics and Space Administration
Moffett Field, Calif., Sept. 15, 1959

A-200.

REFERENCES

1. Wyss, John A., Sorenson, Robert M., and Gambucci, Bruno J.: Effects of Modifications to a Control Surface on a 6-Percent-Thick Unswept Wing on the Transonic Control-Surface Flutter Derivatives. NACA RM A58B04, 1958.

2. Henning, Allen B.: Results of a Rocket-Model Investigation of Control-Surface Buzz and Flutter on a 4-Percent-Thick Unswept Wing and on 6-, 9-, and 12-Percent-Thick Swept Wings at Transonic Speeds. NACA RM L53I29, 1953.

3. Erickson, Albert L., and Stephenson, Jack D.: A Suggested Method of Analyzing for Transonic Flutter of Control Surfaces Based on Available Experimental Evidence. NACA RM A7F30, 1947.

4. Bratt, J. B., Miles, C. J. W., and Johnson, R. F.: Measurements of the Direct Hinge Moment Derivatives at Subsonic and Transonic Speeds for a Cropped Delta Wing with Oscillating Flap. British A.R.C. 19,292 and A.R.C. 0.1335.

5. Martz, C. William: Experimental Hinge Moments on Two Freely Oscillating Trailing-Edge Controls Hinged at 55 Percent Control Chord. NACA RM L57J25, 1957.

6. Reese, David E., Jr., and Carlson, William C. A.: An Experimental Investigation of the Hinge-Moment Characteristics of a Constant-Chord Control Surface Oscillating at High Frequency. NACA RM A55J24, 1955.

7. Gambucci, Bruno J., and Wyss, John A.: Experimental Investigation of the Drag Due to Wedges Along the Trailing Edge of a Swept Wing. NACA RM A58D15, 1958.

8. Levy, Lionel L., Jr., and Knechtel, Earl D.: Experimental Study of the Effect of Sweepback on Transonic Aileron Flutter. NACA RM A51E04, 1951.

[redacted]



TABLE I.- MEASURED FLUTTER DERIVATIVES FOR PLAIN CONTROL SURFACE

| $c_b/c_f = 0.40$; $\alpha = 0^o$; $\delta_m = 0^o$; $\delta_o = \pm 1.08^o$ | | | | | | | | | | | |
|---|---|---|---|---|---|---|---|---|---|---|---|
| M | $\omega$ | k | $\lvert c_{h_\delta} \rvert$ | $\theta$, deg | $kc_{h_\delta}$ | M | $\omega$ | k | $\lvert c_{h_\delta} \rvert$ | $\theta$, deg | $kc_{h_\delta}$ |
| 0.80 | 62.8 | 0.273 | 0.358 | 189 | -0.077 | 0.99 | 62.8 | 0.226 | 0.722 | 156 | 0.169 |
| | | | | | | | 94.2 | .339 | .700 | 164 | .177 |
| .86 | 62.8 | .250 | .328 | 185 | -.053 | | 125.7 | .453 | .740 | 158 | .195 |
| | 94.2 | .375 | .333 | 191 | -.067 | | 157.1 | .566 | .755 | 163 | .276 |
| | 125.7 | .501 | .399 | 191 | -.058 | | 188.5 | .678 | .792 | 152 | .312 |
| | 157.1 | .626 | .366 | 214 | -.152 | | | | | | |
| | 188.5 | .752 | .468 | 214 | -.206 | 1.01 | 62.8 | .220 | .742 | 165 | .128 |
| | | | | | | | 94.2 | .329 | .732 | 163 | .177 |
| .91 | 62.8 | .242 | .382 | 180 | -.019 | | 125.7 | .440 | .716 | 163 | .195 |
| | 94.2 | .363 | .455 | 180 | -.009 | | 157.1 | .549 | .755 | 165 | .223 |
| | 125.7 | .485 | .364 | 175 | .010 | | 188.5 | .659 | .747 | 156 | .288 |
| | 157.1 | .606 | .394 | 180 | 0 | | | | | | |
| | 188.5 | .727 | .409 | 185 | -.058 | 1.03 | 62.8 | .215 | .732 | 166 | .117 |
| | | | | | | | 94.2 | .324 | .758 | 167 | .146 |
| .93 | 62.8 | .239 | .431 | 173 | .037 | | 125.7 | .431 | .761 | 164 | .169 |
| | 94.2 | .357 | .481 | 171 | .097 | | 157.1 | .539 | .780 | 169 | .201 |
| | 125.7 | .477 | .481 | 170 | .155 | | 188.5 | .646 | .810 | 160 | .202 |
| | 157.1 | .596 | .430 | 180 | .057 | | | | | | |
| | 188.5 | .716 | .504 | 178 | .101 | 1.06 | 62.8 | .209 | .824 | 167 | .073 |
| | | | | | | | 94.2 | .314 | .808 | 167 | .125 |
| .95 | 62.8 | .233 | .727 | 153 | .271 | | 125.7 | .419 | .786 | 166 | .171 |
| | 94.2 | .350 | .697 | 159 | .326 | | 157.1 | .523 | .805 | 170 | .190 |
| | 125.7 | .466 | .682 | 151 | .343 | | 188.5 | .628 | .861 | 163 | .200 |
| | 157.1 | .583 | .629 | 152 | .367 | | | | | | |
| | 188.5 | .699 | .559 | 153 | .332 | 1.11 | 62.8 | .203 | .713 | 163 | .116 |
| | | | | | | | 94.2 | .304 | .713 | 167 | .126 |
| .97 | 62.8 | .229 | .841 | 157 | .303 | | 125.7 | .404 | .665 | 165 | .156 |
| | 94.2 | .343 | .822 | 158 | .346 | | 157.1 | .506 | .744 | 170 | .170 |
| | 125.7 | .457 | .770 | 151 | .385 | | 188.5 | .607 | .750 | 163 | .157 |
| | 157.1 | .571 | .788 | 159 | .380 | | | | | | |
| | 188.5 | .686 | .722 | 146 | .444 | 1.14 | 125.7 | .395 | .697 | 166 | .144 |
| | | | | | | | 188.5 | .593 | .744 | 158 | .098 |
| .98 | 62.8 | .225 | .869 | 161 | .205 | | | | | | |
| | 94.2 | .337 | .810 | 158 | .258 | | | | | | |
| | 125.7 | .450 | .779 | 153 | .334 | | | | | | |
| | 157.1 | .562 | .814 | 156 | .356 | | | | | | |
| | 188.5 | .674 | .861 | 145 | .332 | | | | | | |

[redacted]

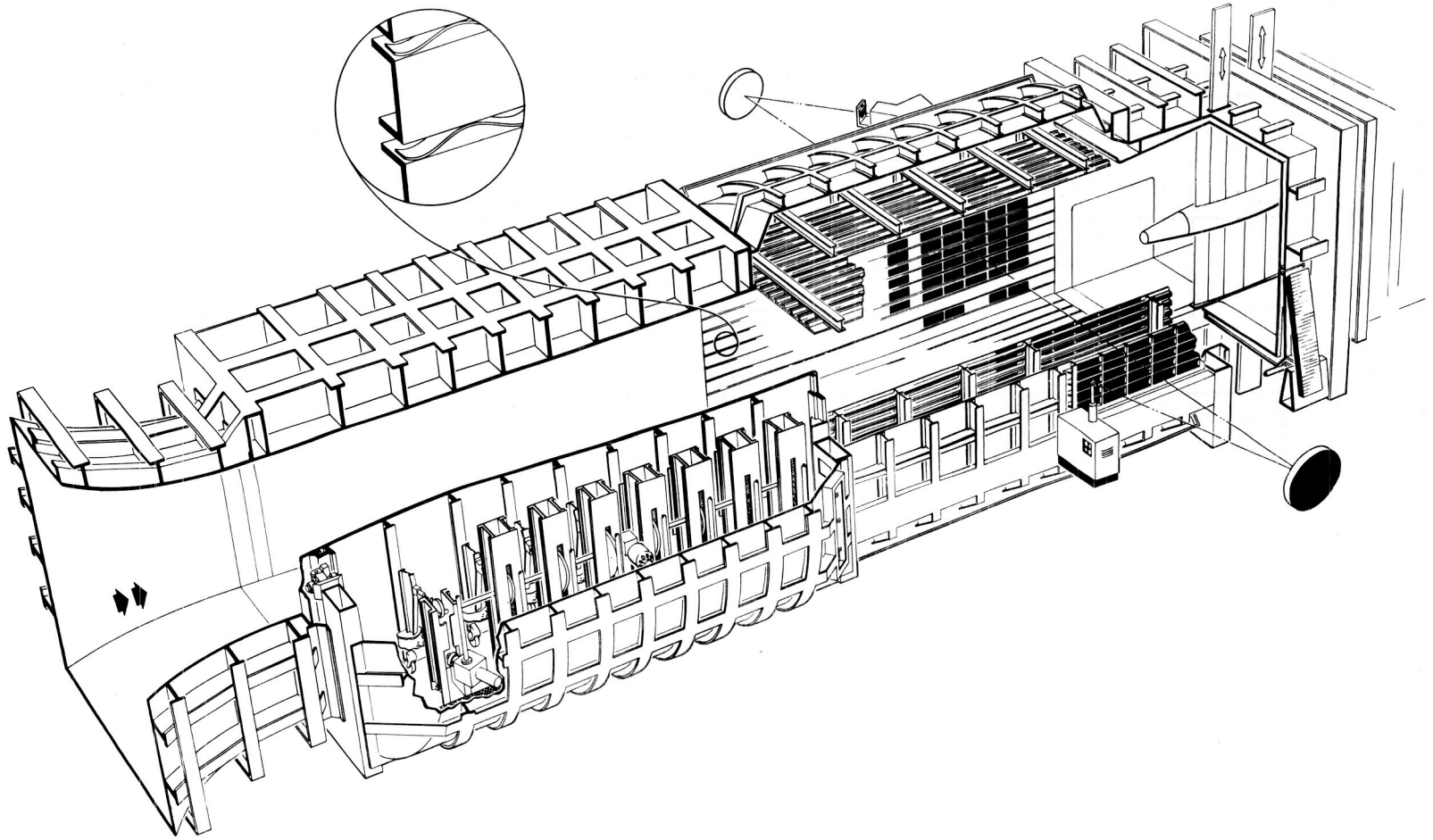

Figure 1.- Sectional sketch of nozzle and test section of Ames 14-foot transonic wind tunnel.

A-23807

Figure 2.- Model mounted in the test section.

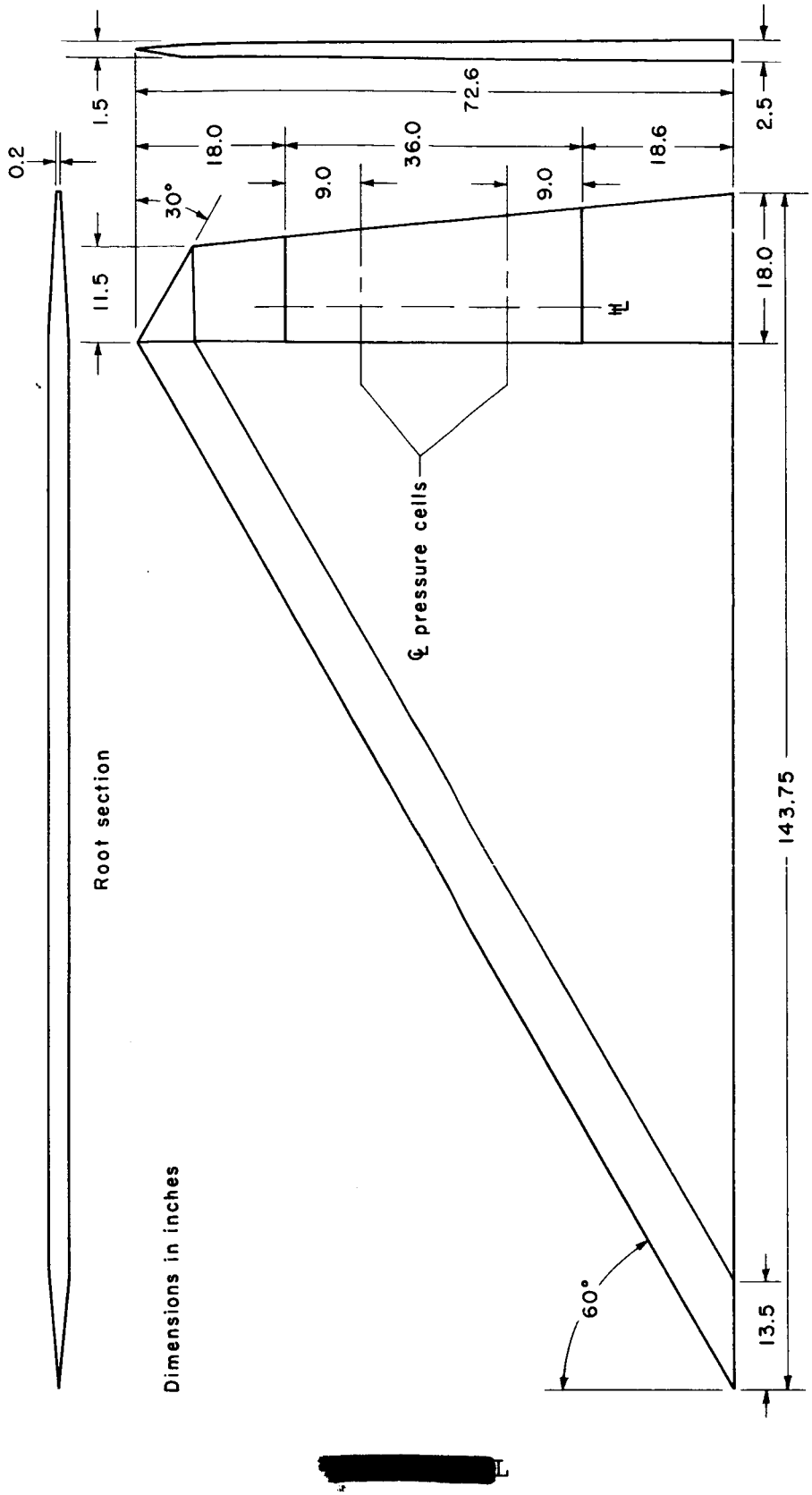


Figure 3.- Model plan form.

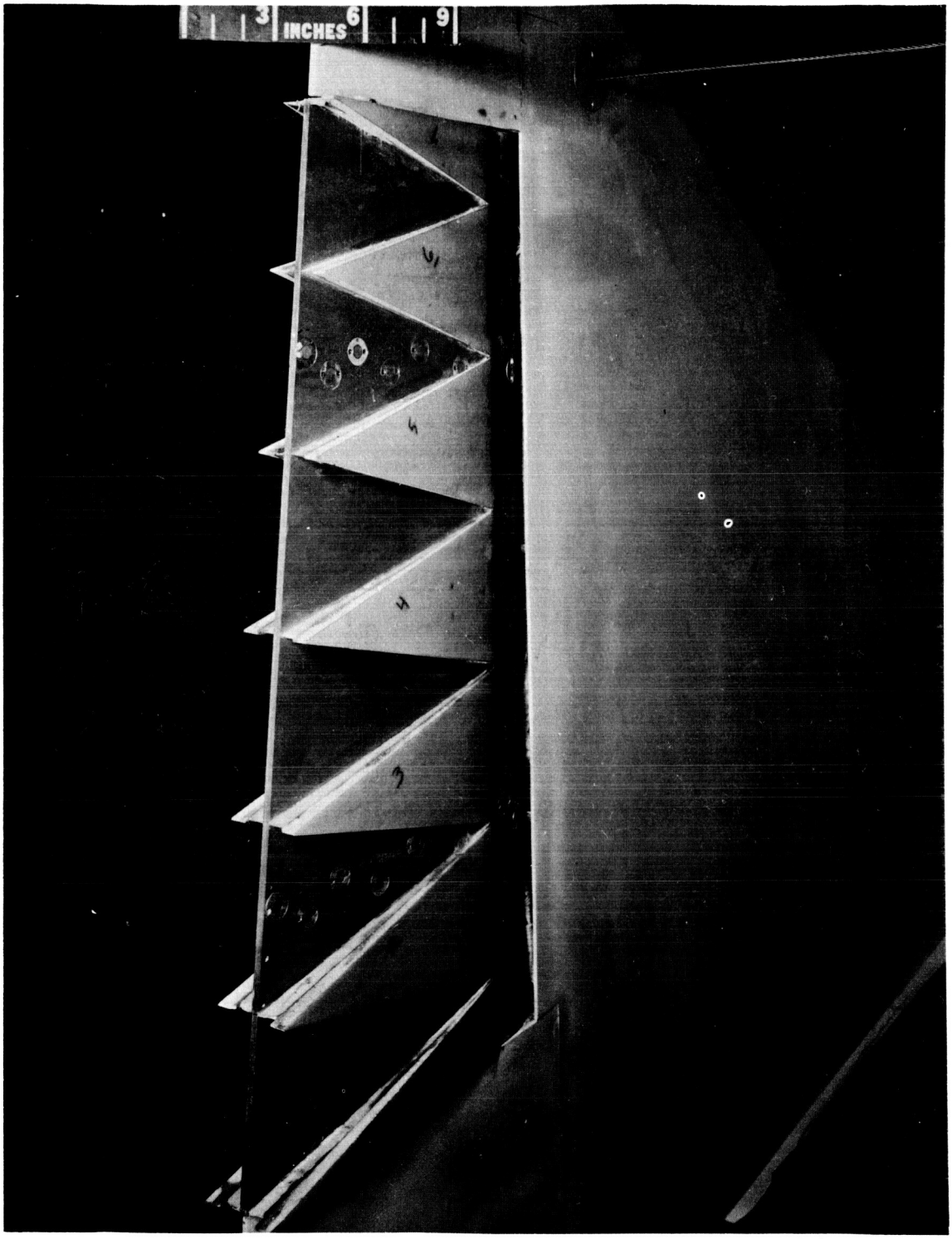


A-23822

Figure 4.- Control surface with wedges having 30° included angle and 3.6° ramp angle.

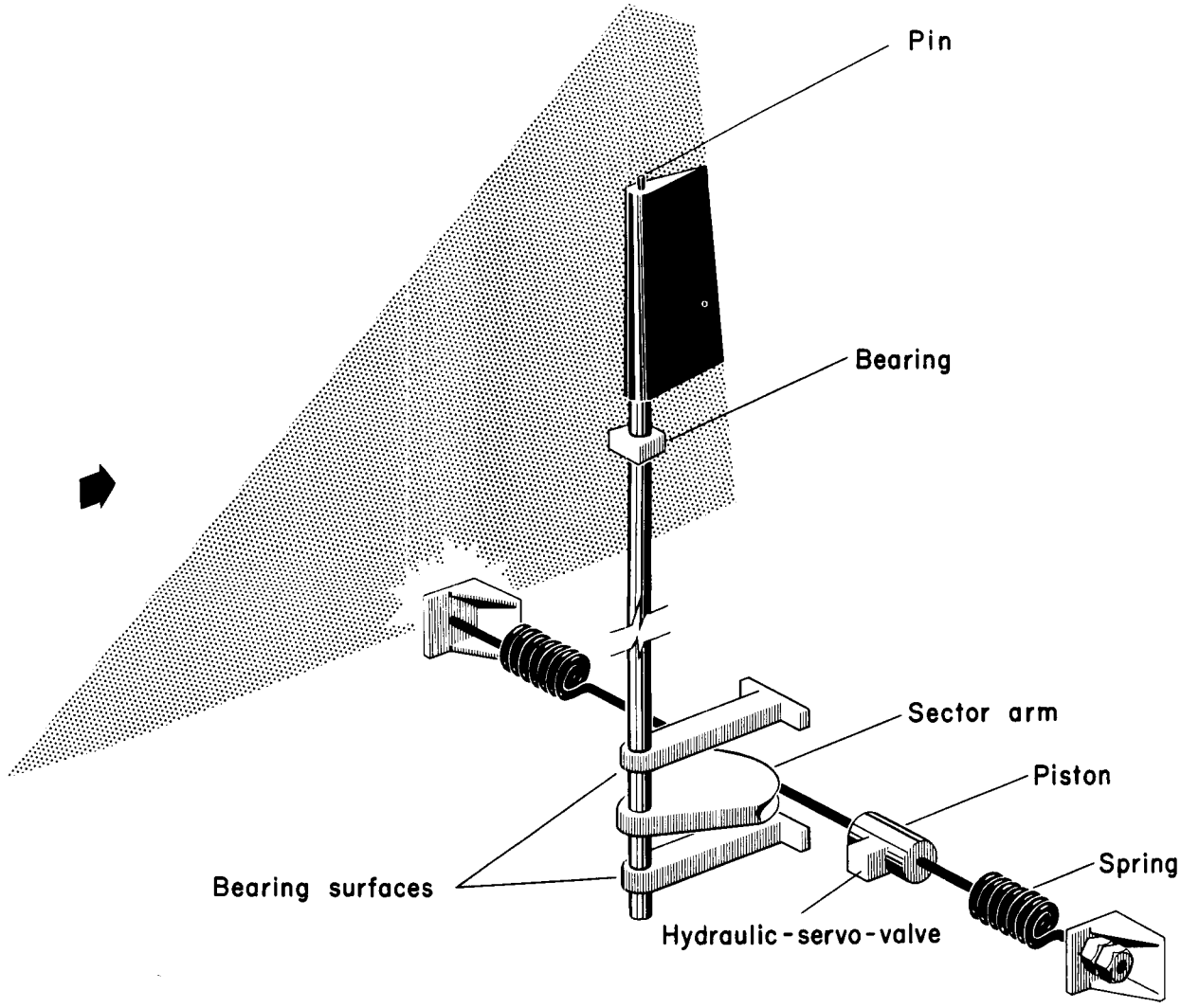


Figure 5.- Schematic drawing of the mechanical details of the control-surface drive system.

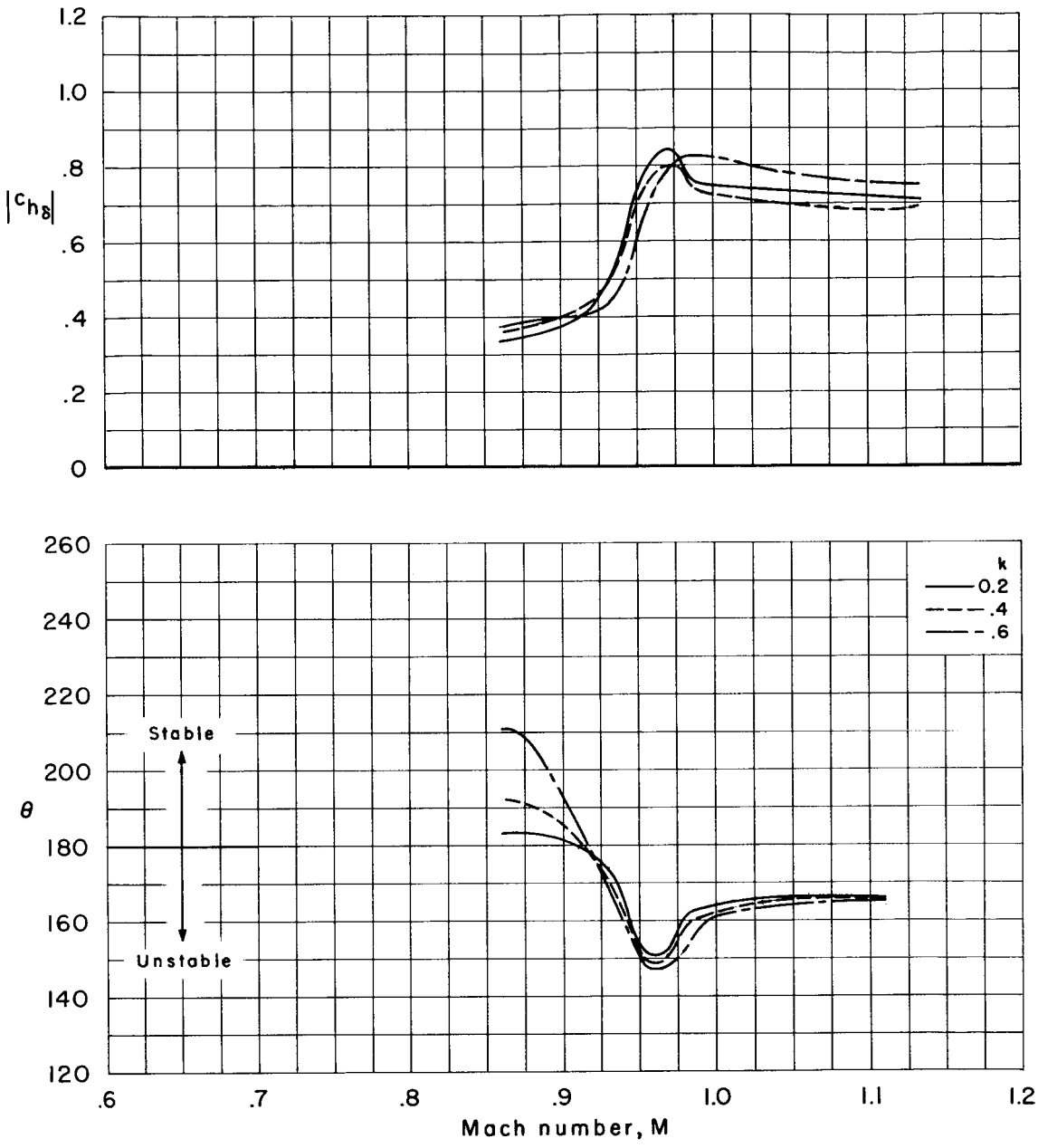


(a) Resultant aerodynamic hinge moment and phase angle as functions of Mach number.

Figure 6.- Effect of reduced frequency for plain control surface.

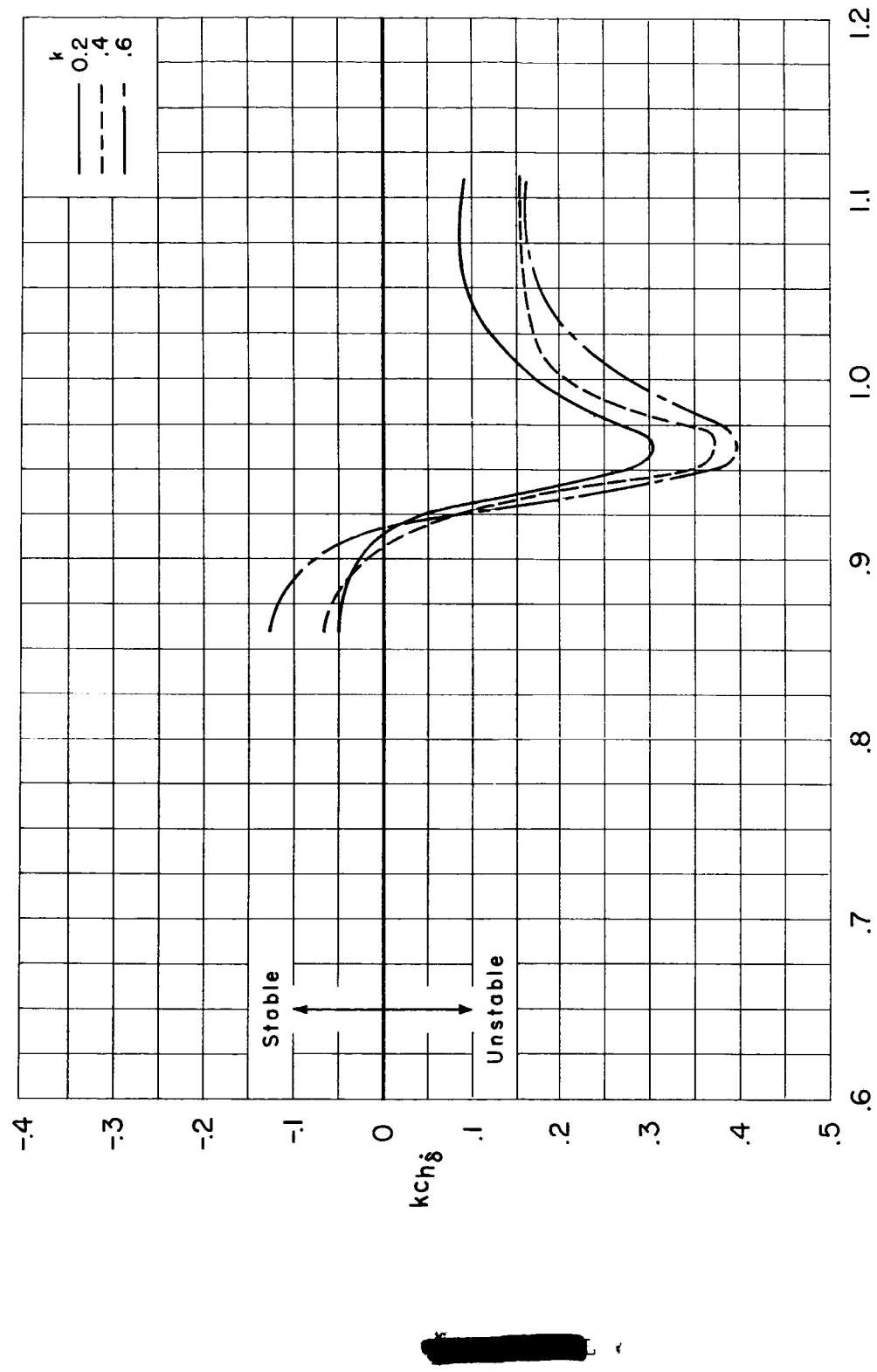


(b) Aerodynamic damping component as a function of Mach number.

Figure 6.- Concluded.

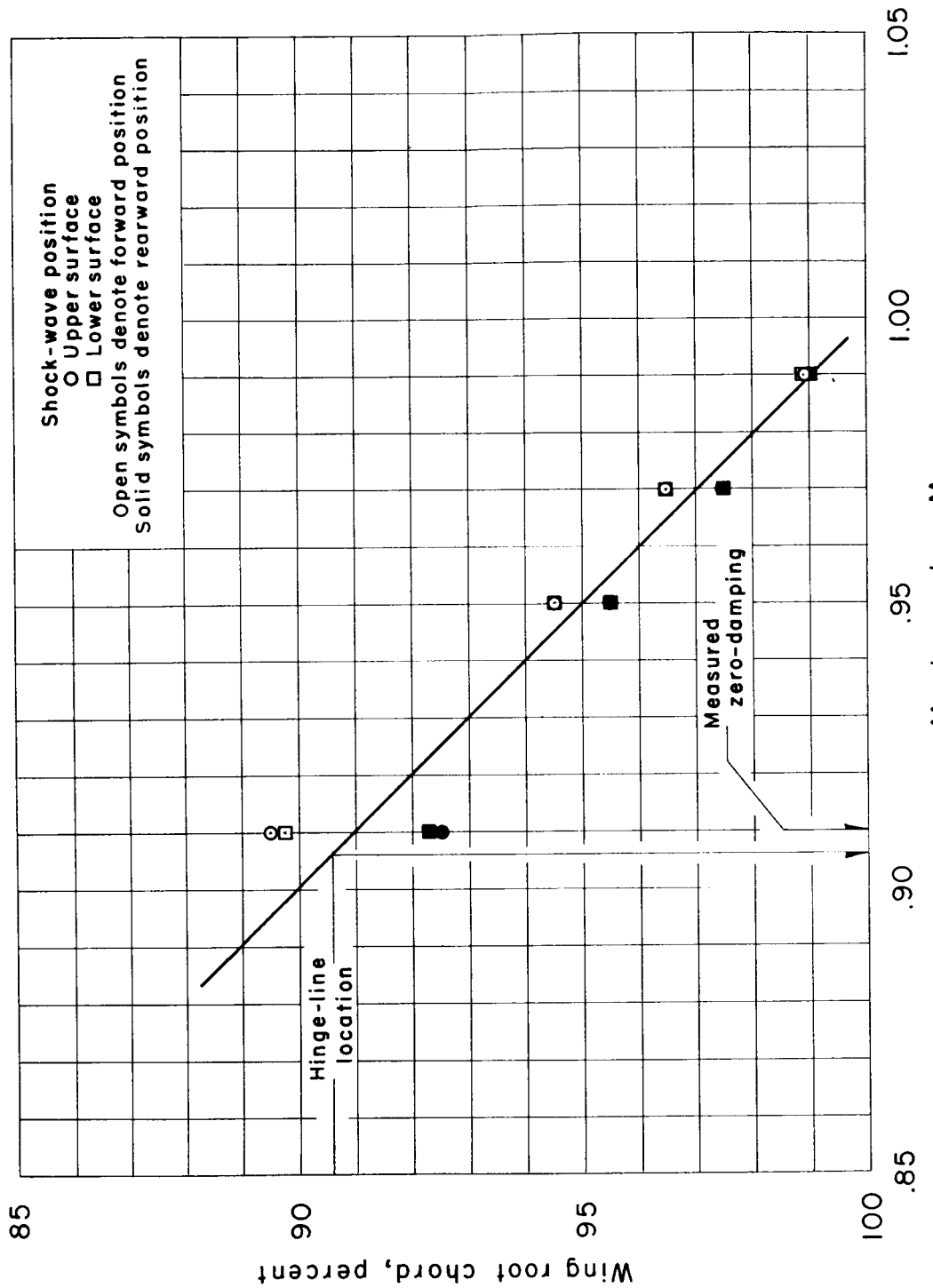


Figure 7.- Location of shock wave as a function of Mach number for the plain control surface.

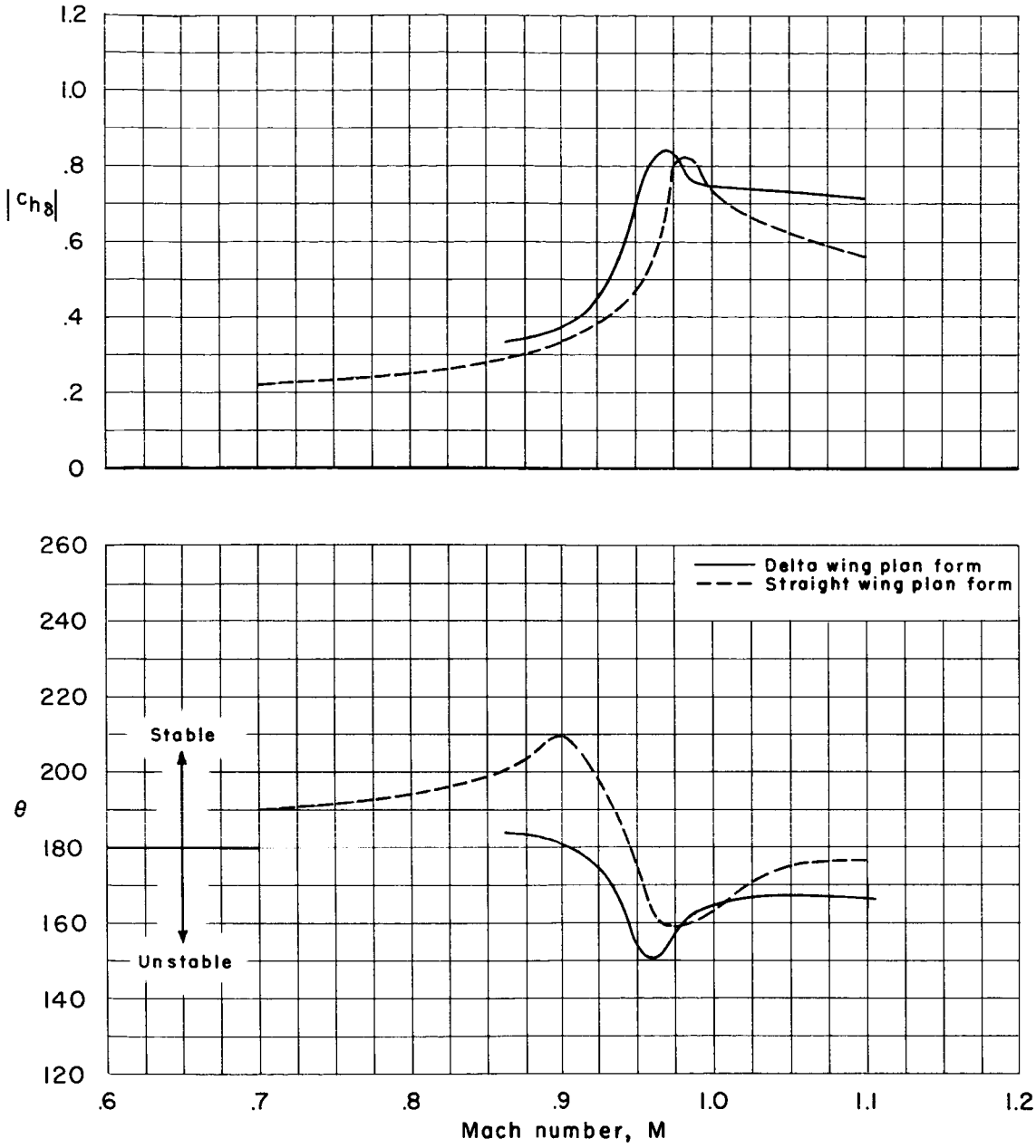


(a) Resultant aerodynamic hinge moment and phase angle as functions of Mach number.

Figure 8.- Comparison of results for straight and delta plan forms; k = 0.2.

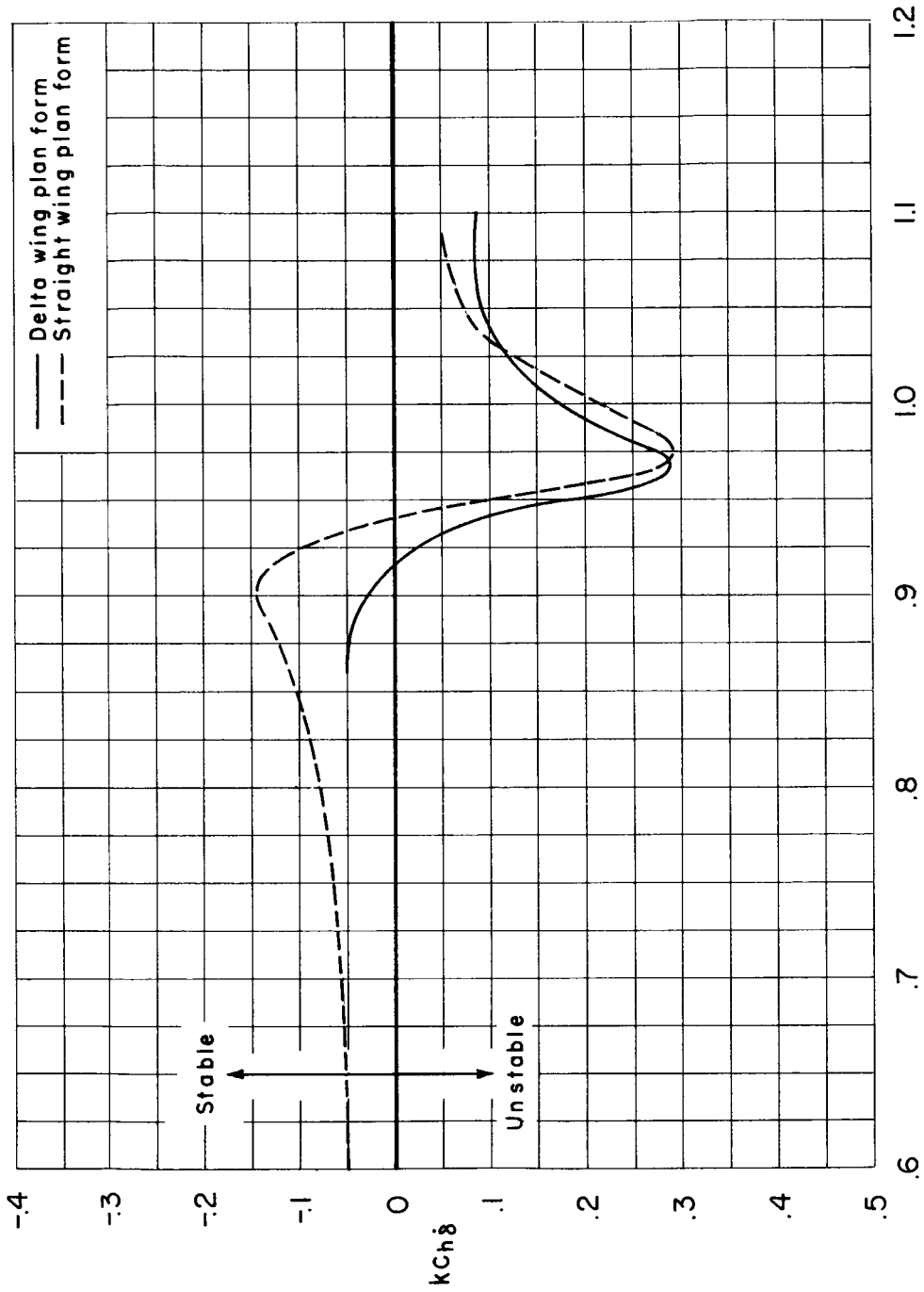


(b) Aerodynamic damping component as a function of Mach number.

Figure 8.- Concluded.